Supporting Information

Microstructure evolution, dielectric relaxation and scaling behavior of Dy-for-Fe substituted Ni-nanoferrites

Ankurava Sinha and Abhigyan Dutta*

Department of Physics, The University of Burdwan, Burdwan-713104, India

***Author for correspondence:**

AbhigyanDutta

Address: Department of Physics, The University of Burdwan, Golapbag, Burdwan-713104, INDIA. **Telephone: +913422657800; Fax: +91342 2634015**

email: adutta@phys.buruniv.ac.in

Theoritical basis of Impedance spectroscopy

For ac analysis we have used complex impedance spectroscopy (CIS) technique which has been carried out in view of its importance in describing the electrical process occurring in a system on applying an AC signal across the sample pellet. The output response of such an experimental measurement, when depicted in a complex plane plot, appears in the form of successive semicircles representing the contributions to the electrical properties due to grain, grain boundary effects and interfacial polarization phenomenon if any. This CIS technique enables us to separate the effects due to each component (grain, grain boundary and electrode polarization effect) in a polycrystalline sample very easily. The impedance measurements on a material give us data having both resistive (real) and reactive (imaginary) components. It can be displayed conventionally in a complex plane plot in terms of some complex parameters like complex impedance (Z^*), complex admittance (Y^*), complex modulus (M^*), complex permittivity (M'') and dielectric loss ($\tan\delta$). These frequency dependent parameters are related to each other by the following relations:

$$Z^* = Z' - jZ'' = R_S - \frac{j}{\omega C_S} = \frac{1}{j\omega C_0 \varepsilon^*}$$

$$Y^* = Y' + jY'' = \frac{1}{R_P} + J\omega C_P = j\omega C_0 \varepsilon^* = \frac{1}{Z^*}$$

$$M^* = M' + jM'' = \frac{1}{\varepsilon^*} = j\omega CoZ^*$$

$$\varepsilon^*(\omega) = \varepsilon' - j\varepsilon''$$

$$\tan\delta = \frac{Z'}{Z''} = \frac{Y'}{Y''} = \frac{M''}{M'} = \frac{\varepsilon''}{\varepsilon'}$$

where R_S and R_P are the series and parallel resistances respectively; C_S and C_P the series and parallel capacitances respectively; Co the geometrical capacitance; Z', Y', M', ε' and Z'', Y'', M'', ε'' denote the real and imaginary components of the impedance, admittance, modulus and permittivity respectively ($j = \sqrt{(-1)}$).

The peak of the high-frequency semicircular arc in the complex impedance spectrum enables us to evaluate the relaxation frequency ($\omega_{\max}$) of the bulk material (effects due to grain) in accordance with the relation:

$$\omega_{max}\tau = \omega_{max}R_bC_b = 1 = 2\pi f_{max}R_bC_b$$

where τ represents relaxation time.

The impedance plot can be analyzed with the help of R-Q network. Here Q is related to R and C by the following equation

$$C = R^{\frac{1-a}{a}} Q^{\frac{1}{a}}$$

where the exponent 'a' lies between 0 and 1. The generalized model for this analysis is shown in Fig s1(a).

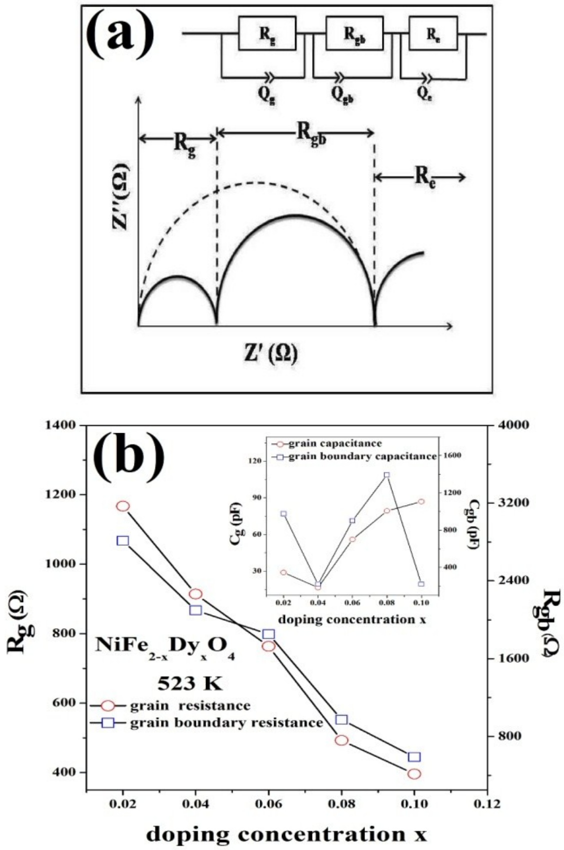

Fig s1:(a) Equivalent circuit model showing contributions from grain, grain boundary and electrode polarization, (b) Variation of grain and grain boundary resistances with doping concentration. Also variation of grain and grain boundary capacitances are shown in the inset.

The DC conductivity of the samples can been evaluated from the resistivity using the following relation –

$$\sigma = \frac{t}{RA}$$

where t is the width of the pellets, A is the area of the pellets and R is the resistance.

The variation of logarithmic conductivity with reciprocal of temperature is normally found to obey the Arrhenius equation given by,

$$\sigma = \frac{\sigma_0}{T} \exp(-\frac{E_a}{kT})$$

where σ_o is pre-exponential factor, E_a is the activation energy of electrical conduction, k is the Boltzman's constant and T is the absolute temperature.

Modulus analysis:

A very effective, important and convenient tool to analyze and interpret the dynamical aspects of electrical transport phenomenon is the complex modulus formalism. It describes the inhomogeneous nature of the polycrystalline ceramics. The dielectric relaxation process can also be represented by complex modulus analysis. It also enables to distinguish between the microscopic processes responsible for localized dielectric relaxation and long range conduction. It gives an emphasis to the electrical process characterized by the smallest capacitance in accordance with the relation

$$M' = \frac{C_0}{C}\frac{(\omega RC)^2}{[1+(\omega RC)^2]}$$

$$M'' = \frac{C_0}{C}\frac{\omega RC}{[1+(\omega RC)^2]}$$

Normally, frequency variation of M' shows a dispersion which shifts towards the higher frequency side with the increase in temperature. In the low frequency region M' approaches to zero and shows a continuous dispersion with the frequency having a tendency to saturate at a maximum asymptotic value in high frequency region for all the temperatures. This may be due to short range mobility of charge carriers. Such results may possibly be related to a lack of restoring force governing the mobility of charge carriers under the action of an induced electric field.

M'' exhibits an asymmetric maxima at the dispersion region of M'. The conductivity relaxation times are obtained from the peak frequency of M''.

Dielectric property analysis:

We have analyzed the dielectric spectra using Havriliak-Negami (H-N) formalism which is in fact a combination of Cole/Cole and Cole/Davidson function. According to this formalism, the generalized dielectric function is given by

$$\varepsilon *_{HN}(\omega) = \varepsilon'(\omega) - i\varepsilon''(\omega) = \varepsilon_\infty + \frac{\varepsilon_s - \varepsilon_\infty}{(1+(i\omega\tau_{HN})^\beta)^\gamma} + \frac{S}{i\omega^p}$$

Where ε_s and ε_∞ are the relaxed and unrelaxed permittivity respectively and their difference $\varepsilon_s - \varepsilon_\infty = \Delta\varepsilon$ represents the dielectric relaxation strength with $\varepsilon_s = \lim_{\omega\tau_{HN} \ll 1} \varepsilon'(\omega)$ and $\varepsilon_\infty = \lim_{\omega\tau_{HN} \gg 1} \varepsilon''(\omega)$ and τ_{HN} is the characteristic relaxation time. The fractional shape parameters β and γ describe the symmetric and asymmetric broadening of the complex dielectric function and should satisfy the conditions $0 \leq \beta \leq 1$ and $0 \leq \beta\gamma \leq 1$. The unity value of β and γ corresponds to ideal Debye relaxation and the non-zero values of them correspond to a distribution of relaxation times.The real and imaginary parts of ε can be separated by the following equations

$$\varepsilon^{'}(\omega) = \varepsilon_{\infty} + \Delta\varepsilon\, R\, [\frac{1}{(1 + (i\omega\tau_{HN})^{\beta})^{\gamma}}]$$

and

$$\varepsilon^{''}(\omega) = \Delta\varepsilon\, Im \left[\frac{1}{\left(1 + \left(i\omega\tau_{HN}\right)^{\beta}\right)^{\gamma}}\right] + \frac{S}{\omega^{p}}$$

Where R and Im represent real and imaginary parts respectively. S is related to dc conductivity arising from ionic conduction and p is the frequency exponent.

Simplified partial output of Rietveld Analysis for the sample $NiFe_{1.94}Dy_{.06}O_4$

Refinement final output indices:

Global Rwp: 0.045509357

Global Rp: 0.03584254

Global Rwpb (no background): 0.06621593

Global Rpb (no background): 0.05134256

Total Energy: 0.0

Refinement final output indices for single samples:

Sample Sample_x :

Sample Rwp: 0.045509357

Sample Rp: 0.03584254

Sample Rwpb (no background): 0.06621593

Sample Rpb (no background): 0.05134256

Refinement final output indices for single datasets:

DataSetDataFileSet_x :

DataSetRwp: 0.045509357

DataSetRp: 0.03584254

DataSetRwpb (no background): 0.06621593

DataSetRpb (no background): 0.05134256

Refinement final output indices for single spectra:

Datafiles25.DAT :Rwp: 0.045509357, Rp: 0.03584254, Rwpb: 0.06621593, Rpb: 0.05134256

Reflection list

n h k l multiplicity meanFhkl crystallite(Angstrom) microstrain

1) 2 2 0 12 288697.0504754523 502.6410947861138 1.4054017532204497E-4

2) 3 1 1 24 1639165.4072002596 521.644079685799 3.51699373780433E-4

3) 2 2 2 8 113673.3687849667 574.3050861039785 5.658683363012102E-4

4) 4 0 0 6 670725.7096088809 587.2491208451836 1.01962105E-4

5) 3 3 1 24 34230.37513970447 494.3284052800255 2.812976352165279E-4

6) 4 2 2 24 378070.8406814843 502.5410947888961 1.4054017532204497E-4

7) 5 1 1 24 1291123.9748478886 563.5448172573716 1.684640544251737E-4

8) 3 3 3 8 319422.5192820907 474.3050861039785 1.6586833630121005E-5

9) 4 4 0 12 2824032.68601315 502.5410947861138 1.4054017532204497E-4

10) 5 3 1 48 107206.9837304948 515.6103330929427 2.208369848049911E-5

11) 4 4 2 24 64.65451235692242 486.8544232956975 2.1123509180992975E-4

12) 6 2 0 24 265944.62467793736 556.7542314639185 1.200438338909842E-4

13) 5 3 3 24 812191.9178056031 489.9425511624346 3.6322661326867856E-4

14) 6 2 2 24 368597.9822778156 534.044079685799 2.31699373780433E-4

15) 4 4 4 8 350378.05288893427 474.3050861039785 5.658683363012102E-5

16) 5 5 1 24 63905.74592080668 599.3169138638474 1.3808421879479514E-4

17) 7 1 1 24 21055.381928131268 474.3523971549264 9.403998703552776E-5

18) 6 4 2 48 417251.8323956432 502.5410947874707 1.4054017532204502E-4

19) 5 5 3 24 697005.8416041334 482.6112259744698 4.692567966505957E-4

20) 7 3 1 48 1086467.1459505686 538.6776701089857 6.744123592947342E-5

Object: Fe1

String informations (CIF term, value) :

_atom_site_type_symbol, Fe3+

_atom_site_constraints,

_atom_type_number_in_cell, 8.0

_atom_site_calc_flag, .

Parameter informations :

- Parameter: default.par:Sample_x:1006116:Atomic Structure:Fe1:_atom_site_occupancy Value: 1, minimum: 0.0, maximum: 1.0 Status: not refinable, only positive values permitted, minimum significant value: 0.0

Object: Ni1

String informations (CIF term, value) :

_atom_site_type_symbol, Ni2+

_atom_site_constraints,

_atom_type_number_in_cell, 0.0

_atom_site_calc_flag, .

Parameter informations :

- Parameter: default.par:Sample_x:1006116:Atomic Structure:Ni1:_atom_site_occupancy Value: 0, minimum: 0.0, maximum: 1.0 Status: not refinable, only positive values permitted, minimum significant value: 0.0

Object: Fe2

String informations (CIF term, value) :

_atom_site_type_symbol, Fe3+

_atom_site_constraints,

_atom_type_number_in_cell, 8.0

_atom_site_calc_flag, .

Parameter informations :

- Parameter: default.par:Sample_x:1006116:Atomic Structure:Fe2:_atom_site_occupancy Value: 0.5, minimum: 0.0, maximum: 1.0 Status: not refinable, only positive values permitted, minimum significant value: 0.0

Object: Ni2

String informations (CIF term, value) :

_atom_site_type_symbol, Ni2+

_atom_site_constraints,

_atom_type_number_in_cell, 8.0

_atom_site_calc_flag, .

Parameter informations :

- Parameter: default.par:Sample_x:1006116:Atomic Structure:Ni2:_atom_site_occupancy Value: 0.5, minimum: 0.0, maximum: 1.0 Status: not refinable, only positive values permitted, minimum significant value: 0.0

Object: O1

String informations (CIF term, value) :

_atom_site_type_symbol, O2-

_atom_site_constraints,

_atom_type_number_in_cell, 32.0

_atom_site_calc_flag, .

Parameter informations :

- Parameter: default.par:Sample_x:1006116:Atomic Structure:O1:_atom_site_occupancy Value: 1., minimum: 0.0, maximum: 1.0 Status: not refinable, only positive values permitted, minimum significant value: 0.0

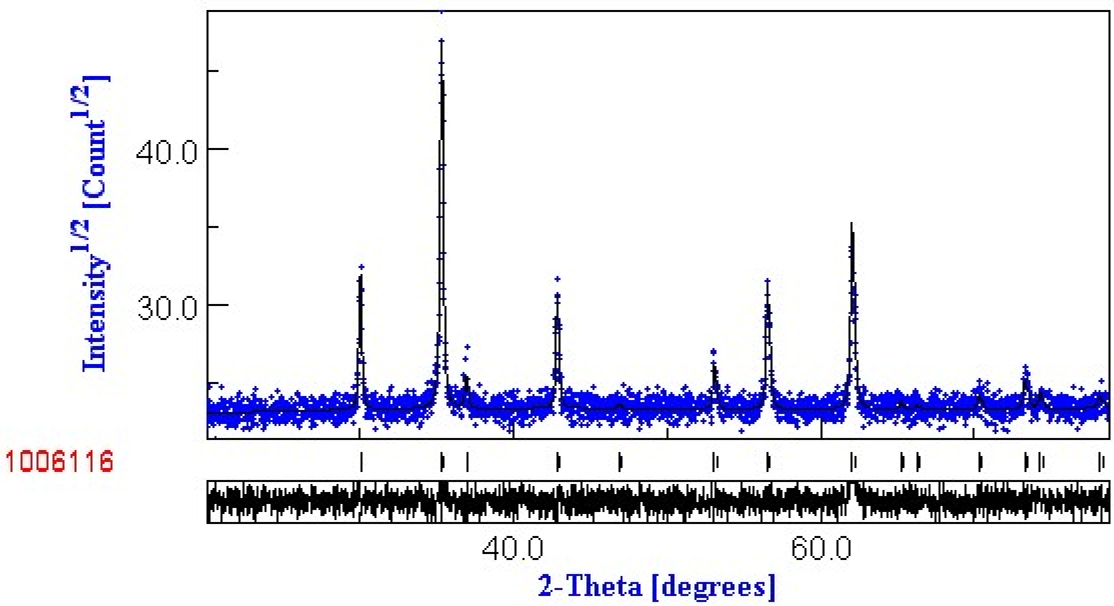

Figure S2: The refined XRD pattern obtained from Rietveld analysis of the sample $NiFe_{1.94}Dy_{.06}O_4$